Structural stability of $Pu_{(1-x)}M_x$ (M=Al, Ga, and In) compounds

G. Robert,[1,*] A. Pasturel,[2] and B. Siberchicot[1]
[1]*Département de Physique Théorique et Appliquée, BP12, 91680 Bruyères-le-Châtel, France*
[2]*Laboratoire de Physique Numérique, CNRS, 25 avenue des Martyrs, BP 106 F-39042 Grenoble, France*
(Received 17 April 2003; published 15 August 2003)

We present results on the structural stability of $Pu_{(1-x)}M_x$ (M=Al,Ga,In) compounds in the framework of density functional theory within the local density approximation and generalized gradient approximation (GGA). An all-electron linear augmented plane wave method, which includes an additional $p_{1/2}$ local orbital in spin orbit coupling, is used in order to determine the formation energy of these compounds. Using the GGA and spin polarized calculations, the calculated structural hierarchy is in agreement with the trends observed in the experimental phases diagrams. The stability of the Pu-M compounds can be related to a strong *pdf* hybridization.

DOI: 10.1103/PhysRevB.68.075109 PACS number(s): 71.15.Ap, 71.15.Nc, 74.70.Ad

I. INTRODUCTION

The actinides series in the periodic table, is characterized by a progressive filling of the $5f$ shell. It can be divided into two sub-series: light actinides (Pa to Np) which present $5f$ delocalized states, and heavy actinides (Am to Lw) with $5f$ localized states. The light actinides have bonding $5f$ electrons and exhibit a band character similar to the *d* electrons in transition metals. In contrast, heavy actinides show localized nonbonding $5f$ electrons rather similar to the $4f$ electrons in lanthanides.

Plutonium metal is located at the boundary between these two different subseries, and this peculiar location results in specific properties such as numerous allotropic forms ($\alpha,\beta,\gamma,\delta,\delta',\epsilon$). Some have very complex open structures (α and β: monoclinic) and others close-packed structures (γ tetragonal and δ and δ' cubic).[1]

The cubic delta phase is ductile and this property makes it convenient for engineering applications. As this phase is only stable from 593 to 736 K, it is stabilized at room temperature by small additions of alloying elements like the IIIB metals Al (Ref. 2) and Ga.[3] Others metals like In (Ref. 4) extend the range of stability of the δ phase and retain it in a metastable state at room temperature under rapid cooling from high temperatures. From phase diagrams considerations, it is clear that the stability of the δ phase depends on those of the Pu_3M (M=Al,Ga,In) compounds. A starting point towards a better understanding of the role of each substituted element on the stability of δ plutonium is the calculation of formation energies of Pu_3M compounds. Particularly, the Pu-In phase diagram is qualitatively simple to understand. It can be viewed as the occurrence of ordered compounds based on the *fcc* underlying lattice, namely, the Pu_3In and the $PuIn_3$ compounds in the L_{1_2} structure and the PuIn compound in the L_{1_0} structure. The Pu-Ga and Pu-Al phase diagrams are more complex (see Table I). If the Pu_3Al and Pu_3Ga compounds are essentially isostructural to the L_{1_2} structure with a slight tetragonal distortion, new ground-state structures appear in the *M*-rich side, namely, the $C15$ and $C32$ structures for $PuAl_2$ and $PuGa_2$, respectively (see Table I). Moreover, for PuM_3 compounds, hexagonal structures like the $D0_{19}$ structure for $PuGa_3$ compound are found to be energetically more favorable than the L_{1_2} structure. Therefore, it seems to be important to compare the stability of the $C15$, $C32$, and $D0_{19}$ structures with superstructures occurring on the *fcc* lattice.

We have undertaken such calculations in the framework of first-principles *DFT* studies. Although standard local density approximation (LDA) energy calculations give accurate results for aluminum, gallium, and indium, the LDA fails to reproduce the equilibrium properties of δ plutonium and to give an energetic stability for Pu_3M compounds.[5] For δ plutonium, numerous approaches have been used to attempt to go beyond the LDA.[6] Recently the LDA+U approach has been successfully applied to determine its structural properties.[7,8] Nevertheless, as the adjustable Hubbard U parameter has been defined for the peculiar case of δ-Pu this method is less attractive in the case of alloys with unknown and variable degrees of $5f$ localization from one phase to the other.

At the same time, Wang and Sun[9] obtained a correct equilibrium volume of δ-Pu by using the generalized gradient approximation (GGA) and by considering an antiferromagnetic alignment of spins. Using the GGA with corrections for spin-orbit coupling and orbital- polarization effects, Söderlind and co-workers[10,11] investigates several magnetic configurations including models for a disordered magnetic structure. The more energetically favorable structure was obtained for the antiferromagnetic type-I ordering and random ordering. An intra-atomic noncollinear magnetism was been considered in plutonium by Nordström and Singh.[12]

Independently on the real physical meaning of magnetism in plutonium which is yet an open question, the introduction of magnetic ordering in calculations leads to major improvements in comparison to the standard nonmagnetic LDA or GGA results. In this paper, we apply this approach to the study of the structural stability of $Pu_{(1-x)}M_x$ compounds and to check its ability to reproduce the major trends of Pu-*M* (M=Al,Ga,In) phase diagrams as discussed above. As antiferromagnetic configurations are difficult to generate in complex alloy structures, we chose to perform all of our alloy

TABLE I. Experimental structures from Refs. 1–4. $SrPb_3$ is a tetragonal distortion of L_{1_2} *Strukturbericht* which leads to L_{6_0}.

Phase	Structure Type	Symmetry	Struktur-bericht	Unit Cell Dimensions (Å)		
				a	*b*	*c*
Pu_3Al	$SrPb_3$	Tetragonal	L_{6_0}	4.499	4.499	4.538
PuAl	CsCl	Cubic	$A12$	10.769	10.769	10.769
$PuAl_2$	Cu_2Mg	Cubic	$C15$	7.874	7.874	7.874
$PuAl_3$	Pu_3Al	Hexagonal	$C36$	6.084	6.084	14.427
Pu_3Ga ζ	$AuCu_3$	Cubic	L_{1_2}	4.507	4.507	4.507
PuGa		Tetragonal	L_{1_0}	6.640	6.640	8.066
$PuGa_2$	AlB_2	Hexagonal	$C32$	4.258	4.258	4.138
$PuGa_3$	Ni_3Sn	Hexagonal	$D0_{19}$	6.300	6.300	4.514
Pu_3In	$AuCu_3$	Cubic	L_{1_2}	4.702	4.702	4.702
PuIn	AuCu	Tetragonal	L_{1_0}	4.811	4.811	4.538
$PuIn_3$	$AuCu_3$	Cubic	L_{1_2}	4.607	4.607	4.607

calculations with a simple ferromagnetic ordering including pure δ-Pu.

In Sec. II the details of the electronic structure calculations are presented. Section III contains the results and their discussion. A brief summary and the conclusions of this work are given in Sec. IV.

II. COMPUTATIONAL DETAILS

The electronic structures and total energies are calculated using the all-electron full-potential linear augmented plane-wave (FP-LAPW) method.[13] The self-consistent calculations are performed with a fully relativistic treatment of the core states and a scalar-relativistic treatment including spin-orbit coupling (SOC) for the valence states. The generalized gradient approximation GGA (Ref. 14) is used and magnetic configurations are taken into account. The basis sets are standard[5] and include $6s$, $6p$, $7s$, $7p$, $6d$, and $5f$ partial waves for Pu, $3s$ and $3p$ for Al, $3d$, $4s$, and $4p$ for Ga, and $4d$, $5s$, and $5p$ for In.

It has been shown[15] that such a method used in the framework of scalar-relativistic treatment including spin-orbit interaction introduces a sensitivity of equilibrium properties with respect to muffin-tin radii. To suppress this dependence which originate from the missing of $p_{1/2}$ radial basis functions, the new extension developed by Kunes *et al.*[16] is used. Additional $p_{1/2}$ local orbitals are included in the basis set. Then this set is well adapted to a correct treatment of $6p$ semicore states modified by SOC. Moreover, in order to obtain more flexibility in the radial basis functions and to decrease the basis set size, new local orbitals $(\mathrm{APW}+lo)$ for $5f$ partial waves of Pu are included.[17]

For $D0_{19}$, $D0_{22}$, L_{1_0}, and L_{1_2} structures (*Strukturbericht*), we used 20 k points in the irreducible Brillouin zone. For 40 and $C15$ structures, we used 40 k points, 126 k points for $C32$, 189 k points for L_{1_1}, and finally 270 k points for δ-plutonium.

All structures have been calculated with a muffin tin radius of 2.5 Bohr excepted for $C32$ (2.2 Bohr). This difference in radius is related to a shorter distance between first neighbors atoms in this peculiar structure. Nevertheless as written above, these differences have no influence on final results. Finally we used $k_{\max}R_{mt}=10$ for planes waves convergence (where R_{mt} is the atomic sphere radius, and $k_{\max}$ is the plane wave cutoff) and a cutoff energy E_{cut} in second-variational-step equals 60 eV for spin-orbit coupling.

III. RESULTS AND DISCUSSION

As already mentioned in Sec. I, magnetic interactions coupled with the GGA improve the structural properties of δ-Pu. In a first step, we tested the influence of different ap-

TABLE II. Experimental and theoretical results for equilibrium volume of δ-Pu.

Element	Approximation used	Theoretical results		Experimental results
		LSDA	GGA	
Pu fcc	nonmagnetic without SOC	16.59	18.05	
Pu fcc	ferromagnetic without SOC	19.34	27.80	24.92[a]
Pu fcc	nonmagnetic with SOC	17.59	19.60	
Pu fcc	ferromagnetic with SOC	18.19	25.51	
Pu fcc	antiferromagnetic with SOC	19.41	23.47	
Al fcc		15.83	16.61	16.6[b]
Ga fcc		17.90	19.82	19.6[c]
In fcc		24.90	27.79	26.1[d]

[a] δ-Pu at 320 °C from Ref. 1.
[b] from Ref. 22.
[c] orthorhombic phase from Ref. 22.
[d] tetragonal phase with $c/a=1.52$ from Ref. 22.

TABLE III. Formation energy $E^f_{Pu_{1-x}M_x}$ using the LDA for Pu-Al alloys (in eV/atom).

Element	non-magnetic without SOC	ferro-magnetic without SOC	non-magnetic with SOC	ferro-magnetic with SOC
L_{1_2}PuAl$_3$	0.068	−0.269	−0.144	−0.283
L_{1_0}PuAl	0.211	−0.239	−0.045	−0.231
L_{1_2}Pu$_3$Al	0.030	−0.159	−0.124	−0.136

proximations on the equilibrium properties of pure δ plutonium. The results are summarized in Table II. The most stable configuration is obtained for an antiferromagnetic-type configuration, followed by ferromagnetic order ($\Delta \sim 0.2$ eV/atom). Nevertheless in both cases the resulting net magnetic moment per atom is weak due to a cancellation of the spin moment by the orbital moment. Let us emphasize that all the results are in complete agreement with previous calculations.[9–11]

For each compound, the total energies provided by the LAPW method are obtained for different values of the volume; let us mention that at each volume, each structure is optimized with respect to all degrees of freedom allowed by its space-group symmetry. A fit based on Murnaghan's equation of state determines the equilibrium total energy and the equilibrium volume. Since the total energies of the pure metals are treated in the same way, the formation energy of an alloy is obtained by substracting the weighted sum of total energies of the constituent elements from the total energy of the compounds:

$$E^f_{Pu_{(1-x)}M_x} = E^{min}_{Pu_{(1-x)}M_x} - ((1-x)E^{min}_{Pu} + xE^{min}_{M}).$$

It should be noted that the *fcc* structure is used for pure Pu, Al, Ga, and In even if the ground states of Pu and Ga are different. Taking into account the orthorhombic structure for the Ga ground state lowers the relevant formation energies of PuGa compounds by ~0.1 eV/atom per Ga atom.

As for δ plutonium, we examine the consequences of different approximations on formation energies of the prototype Pu$_3$Al, PuAl, and PuAl$_3$, compounds in the L_{1_2}, L_{1_0}, and L_{1_2} structures, respectively (see Tables III and IV). Total energy calculations performed without magnetic interactions but including spin-orbit coupling corrections lead to formation energies of Pu$_3$Al in good agreement with previous results[5] (see Table III). The formation energies calculated

TABLE IV. Formation energy $E^f_{Pu_{1-x}M_x}$ using the approximation for Pu-Al alloys (in eV/atom).

Element	non-magnetic without SOC	ferro-magnetic without SOC	non-magnetic with SOC	ferro-magnetic with SOC
L_{1_2}PuAl$_3$	−0.046	−0.329	−0.239	−0.362
L_{1_0}PuAl	0.086	−0.336	−0.135	−0.348
L_{1_2}Pu$_3$Al	−0.049	−0.278	−0.148	−0.257

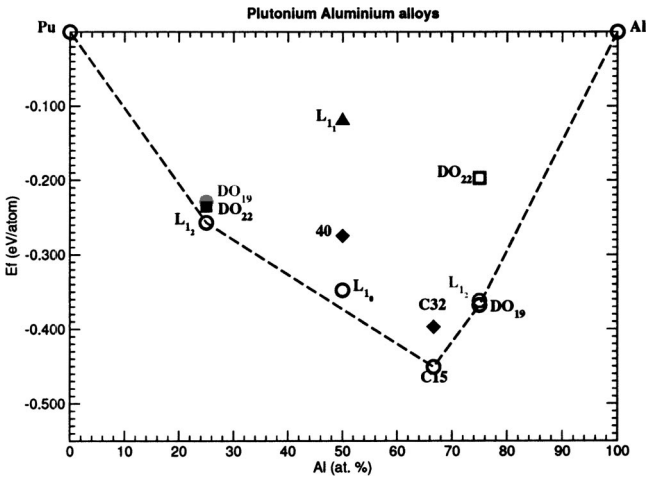

FIG. 1. Formation energies of Pu-Al alloys for several structures using the GGA+spin polarization.

with the GGA vary only slightly from the LDA. Including magnetic interactions leads to much more negative values of all prototype structures, the strongest variation being with GGA (see Table IV). The effect of magnetic interactions is to increase the stability of PuAl compounds in agreement with experimental data.[18] In the same way, the calculated volume of the Pu$_3$Al compound using the GGA and ferromagnetic order, i.e., $V \cong 24$ Å^3/atom, is in close agreement with the experimental value, $V \cong 23$ Å^3/atom, keeping in mind that the ground state structure of the Pu$_3$Al compound is only a slight tetragonal distortion of the L_{1_2} structure.

In Figs. 1–3 we report the formation energies of the *fcc* superstructures as well as the formation energies of the $C15$, $C32$, and $D0_{19}$ structures. As seen in Sec. I, the Pu-In phase diagram is characterized by the occurrence of the L_{1_2} and L_{1_0} structures as ground states while in the Ga-rich side of the Pu-Ga system, the $C32$ and $D0_{19}$ structures are the most stable structures. In the Al-rich side of the Pu-Al system, the $C15$ structure is the ground state while a more complex hexagonal structure than $D0_{19}$ is found to be the most stable

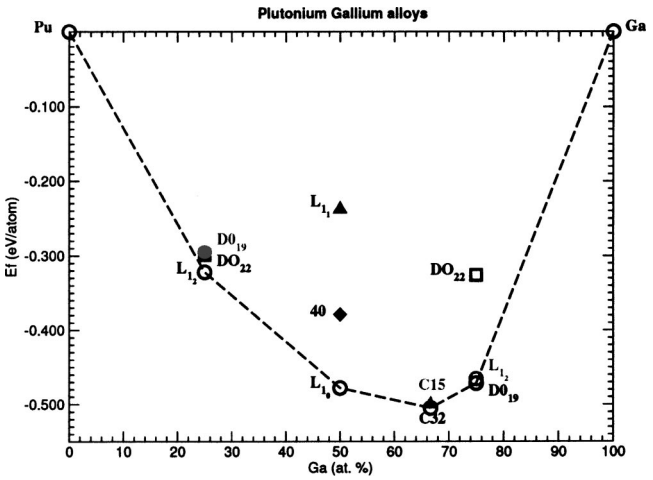

FIG. 2. Formation energies of Pu-Ga alloys for several structures using the GGA+spin polarization.

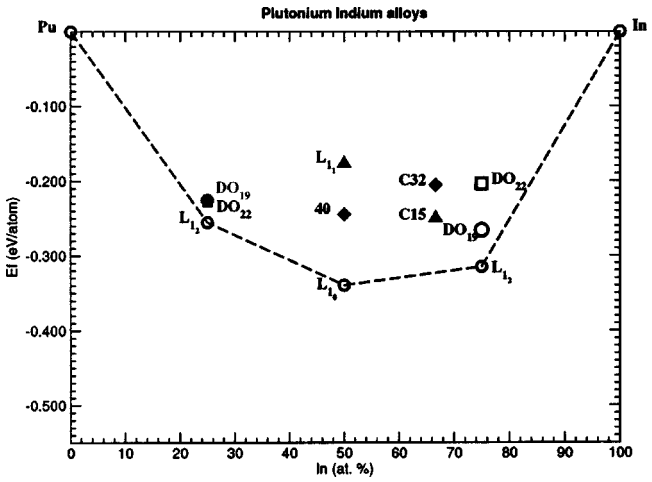

FIG. 3. Formation energies of Pu-In alloys for several structures using the GGA+spin polarization.

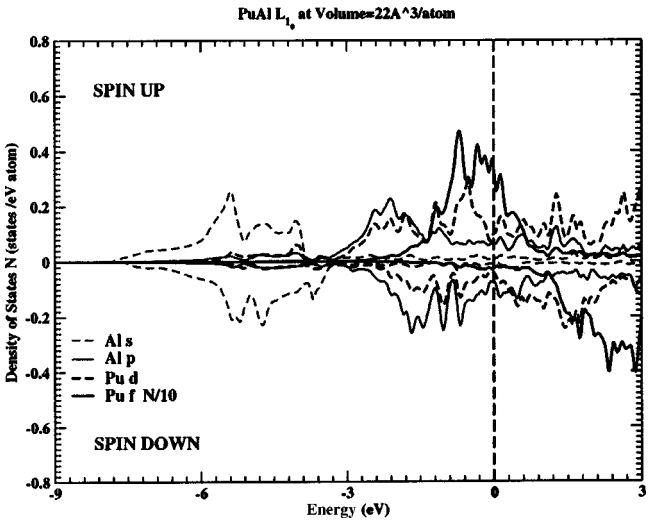

FIG. 5. *l*-projected DOS near theoretical equilibrium volume using the GGA+spin polarization. The Fermi level is set at 0.

structure for the $PuAl_3$ compound. For simplicity, the $D0_{19}$ structure is kept as an hexagonal prototype structure. From Fig. 3, Pu_3In in the L_{1_2} structure, PuIn in the L_{1_0} structure and $PuIn_3$ in L_{1_2} structure are found to be the ground state. On the contrary, by comparing the stability of all the studied structures in the Pu-Ga system, $PuGa_2$ in the $C32$ structure and $PuGa_3$ in the $D0_{19}$ structure are found to be the most stable phases in the Ga-rich side (Fig. 2). At the end, in the Pu-Al system, $PuAl_2$ in the $C15$ structure and the prototype hexagonal $D0_{19}$ structure are the most stable phases in the Al-rich side (Fig. 1). All the present results are in agreement with the experimental facts (Table I) and we can conclude that both the GGA and ferromagnetic order are able to reproduce the different structural hierarchies observed in the three systems.

In order to gain insight at the microscopic level into the phase stability of $Pu_{(1-x)}M_x$ compounds we inspect the partial densities of states (DOS) of Pu_3Al PuAl, and $PuAl_3$ compounds in Figs. 4, 5, and 6, respectively. The total DOS are decomposed into contributions from each angular momentum channel of the constituent atoms. The DOS of δ plutonium calculated near the equilibrium volume is reported for comparison (Fig. 7). For δ plutonium, the main difference between the LSDA[19] and spin polarized GGA is a split of $5f$ states which appears when the gradient correction term is taken into account. In the compounds, although the DOS are dominated by these split $5f$ bands, the binding properties are mainly governed by hybridization between $6d$ and $5f$ states for Pu and $3s$ and $3p$ states for aluminum.

With respect to the DOS of δ plutonium the energy range calculated in PuAl compounds is expanded towards low energies: the bottom of the valence band is located around 4 eV below the Fermi level for plutonium, 7 eV for Pu_3Al, 7.8 eV for PuAl and 9 eV for $PuAl_3$. The most striking feature is the presence of a gap in the bottom area of the DOS and its concentration-dependent location and width. Moreover plu-

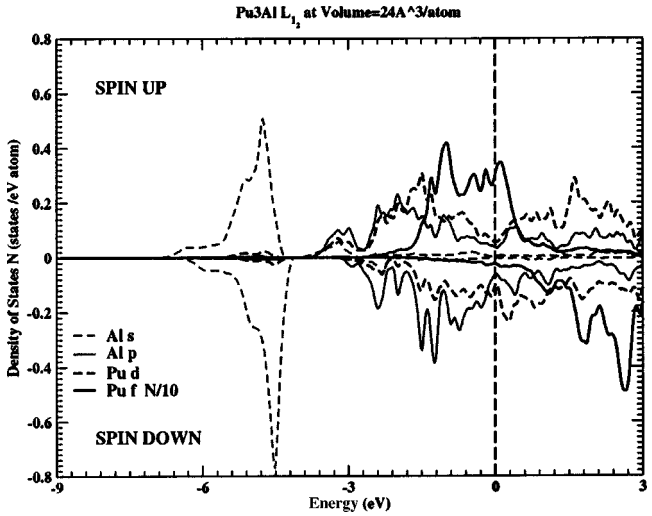

FIG. 4. *l*-projected DOS near theoretical equilibrium volume using the GGA+spin polarization. The Fermi level is set at 0.

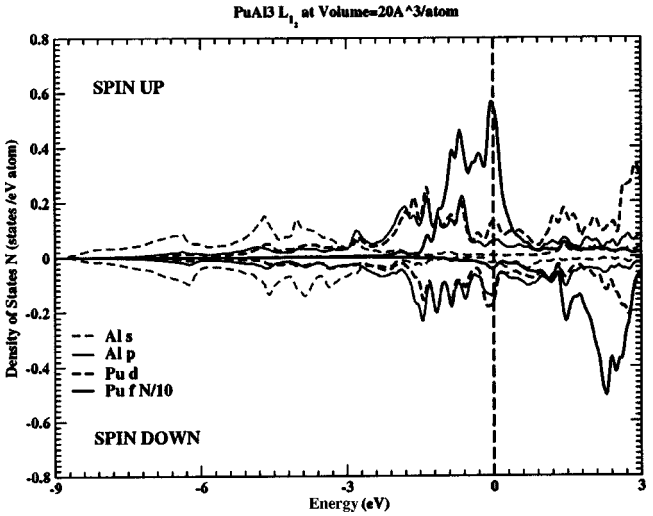

FIG. 6. *l*-projected DOS near theoretical equilibrium volume using the GGA+spin polarization. The Fermi level is set at 0.

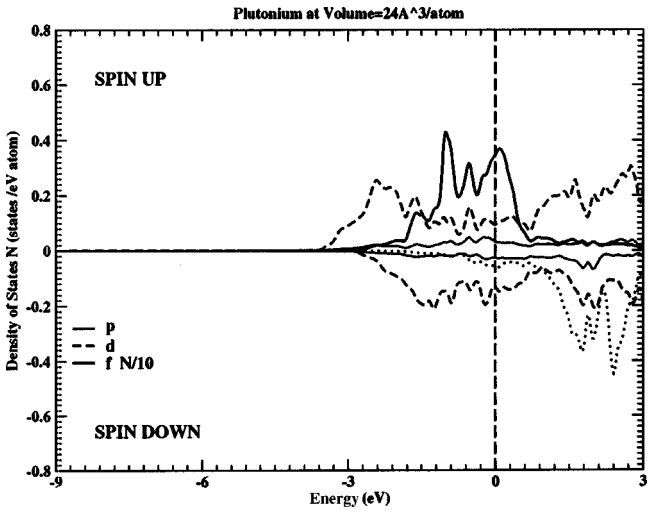

FIG. 7. *l*-projected DOS near theoretical equilibrium volume using the GGA+spin polarization. The Fermi level is set at 0.

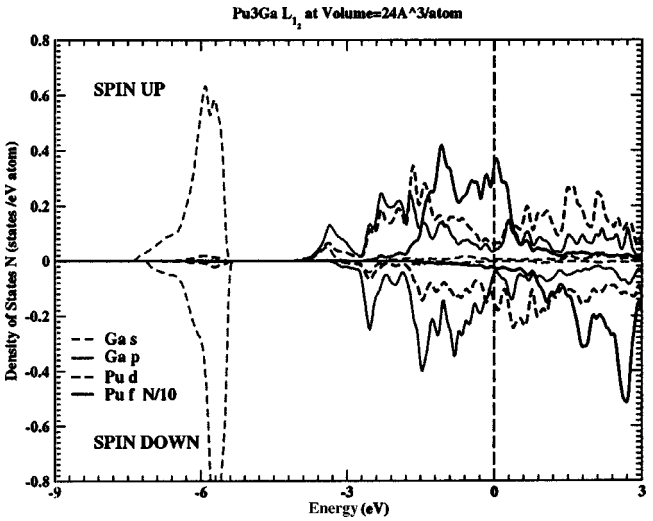

FIG. 8. *l*-projected DOS near theoretical equilibrium volume using the GGA+spin polarization. The Fermi level is set at 0.

tonium $5f$ states become more and more localized with increasing aluminum concentration. Depending on the Al amount, an overlap of $3p$ states of Al and $6d$ states of Pu is observed.

As a starting point, the bonding effects could be analyzed on the basis of the local first-neighbor environment of each atom. For plutonium rich compounds, aluminum is only surrounded by plutonium atoms. As the $3s$ states are only weakly hybridized with Pu states, this $3s$ states becomes localized in an atomiclike configuration leading to an opening of a gap in its originally metallic *sp* states. This feature is enhanced by a greater first-neighbor distance in the compounds ($d_{\text{Al-Pu}}$=3.24 Å in Pu_3Al) than in pure aluminum ($d_{\text{Al-Al}}$=2.86 Å). Then the gap is smaller in PuAl and disappears in $PuAl_3$, as aluminum is now mainly surrounded by other Al atoms, restoring the metallic *sp* band character. Moreover, for the three compounds, the gap width is greater for spin down channel than for spin up channel due to different spin-polarized $3p_{\text{Al}}$-$6d_{\text{Pu}}$ bands.

In a similar way, plutonium neighboring governs the competition between $3p_{\text{Al}}$-$6d_{\text{Pu}}$ and $6d_{\text{Pu}}$-$5f_{\text{Pu}}$ interactions and the localization of $5f$ bands. In Pu_3Al, plutonium is mainly surrounded by plutonium atoms and a strong $6d$-$5f$ hybridization leads to a broad $5f$ band. In $PuAl_3$, the absence of Pu-Pu first-neighbors interactions leads to a weaker overlap of plutonium $6d$ and $5f$ orbitals and then to more localized $5f$ states.

In order to summarize, hybridization effects between Al and Pu are governed by three kinds of first-neighbor interaction competitions depending on the Al amount: Pu($5f$)-Pu($6d$), Al($3p$)-Pu($6d$) and Al($3s$,$3p$)-Al($3s$,$3p$) interactions. All these features still exist in the more complex structures as the $C15$, $C32$ and $D0_{19}$ ones. Let us mention that our results are quite different from those of Ref. 5, since their calculated LDA DOS are nonmagnetic ones. However, it may be emphasized that the main effect of spin polarization is to push the occupied $5f$ and $6d$ states to lower energies. Therefore, hybridization with the wide Al-*sp* band occurs at lower energies which explains the more negative formation energies as seen in Table IV.

The partial DOS for Pu_3Ga and Pu_3In are reported in Figs. 8 and 9. They display the same general trends already observed in Pu_3Al. The main difference comes from the gap widths: respectively 0.5, 1.5, and 1.0 eV for Al, Ga, and In compounds. The gap widths seem directly related to *sp* bands obtained at Pu_3M volume for the pure metals. Although Al and In exhibit broad parabolic *sp* bands, Ga shows a separation between $4s$ and $4p$ states around 2.5 eV below the Fermi level. This behavior favors a larger gap in the alloys for which there is no first- neighbor Ga-Ga interaction.

IV. CONCLUSION

In this work, we have applied first-principles GGA FP-LAPW calculations with a ferromagnetic ordering to describe formation energies of $Pu_{(1-x)}M_x$ (M=Al, Ga, and In) compounds. The validity of these approximations, already

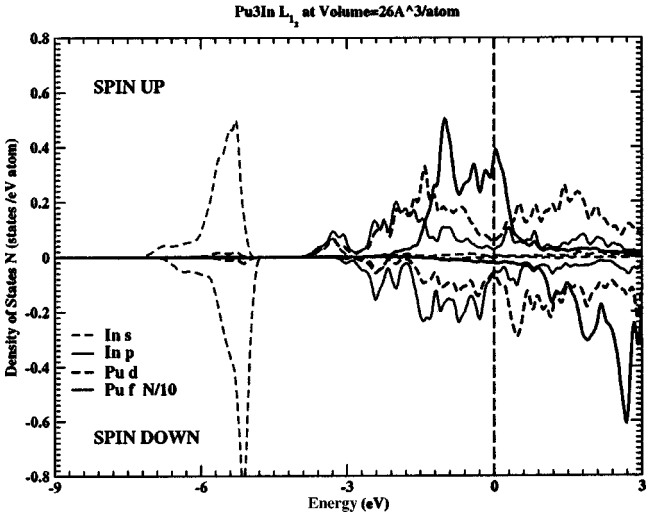

FIG. 9. *l*-projected DOS near theoretical equilibrium volume using the GGA+spin polarization. The Fermi level is set at 0.

used for δ plutonium,[9–11] was successfully checked for these compounds. We have shown the weak effect of spin-orbit coupling on formation energies, the main effect being due to the ferromagnetic-type ordering.

The bonding properties and chemical stability were discussed on the basis of densities of states. As a consequence of local atomic environment, structural stability is governed by the competition between Pu($5f$)-Pu($6d$), $M(p)$-Pu($6d$), and $M(s,p)$-$M(s,p)$ interactions. In the near future, we plan to carry on calculations of several ordered compounds all based on a *fcc* underlying structure in order to perform an accurate Ising-like cluster expansion[20] and to study the stability of the δ phase as a function of temperature and composition.[21]

ACKNOWLEDGMENTS

The authors wish to thanks F. Boucher (Institut des Matériaux Jean Rouxel, Nantes) and P. Novak (Institute of Physics, Praha 6) for their advices concerning the use of the WIEN2K code and for fruitful discussions.

*Electronic address: gregory.robert@cea.fr

[1] *Plutonium Handbook, A Guide to the Technology*, edited by O. J. Wick (American Nuclear Society, LaGrange Park, IL, 1980), Vol. 1.
[2] M. E. Kassner and D. E. Peterson, Bull. Alloy Phase Diagrams **10**, 459 (1989).
[3] M. E. Kassner and D. E. Peterson, Bull. Alloy Phase Diagrams **2**, 1843 (1990).
[4] H. Okamoto, Bull. Alloy Phase Diagrams **2**, 2278 (1990).
[5] J. D. Becker, J. M. Wills, L. Cox, and B. R. Cooper, Phys. Rev. B **54**, R17265 (1996).
[6] M. Pénicaud, J. Phys.: Condens. Matter **12**, 5819 (2000).
[7] J. Bouchet, B. Siberchicot, F. Jollet, and A. Pasturel, J. Phys.: Condens. Matter **12**, 1723 (2000).
[8] S. Y. Savrasov and G. Kotliar, Phys. Rev. Lett. **84**, 3670 (2000).
[9] Y. Wang and Y. F. Sun, J. Phys.: Condens. Matter **12**, L311 (2000).
[10] P. Söderlind, Europhys. Lett. **55**, 525 (2001).
[11] P. Söderlind, A. Landa, and B. Sadigh, Phys. Rev. B **66**, 205109 (2002).
[12] L. Nordström and D. J. Singh, Phys. Rev. Lett. **76**, 4420 (1996).
[13] P. Blaha, K. Schwarz, G. Madsen, D. Kvasnicka, and J. Luitz, WIEN2K, Techn. Universität Wien, Austria, (2001).
[14] J. P. Perdew and D. J. Singh, Phys. Rev. B **46**, 6671 (1992).
[15] L. Nordström, J. M. Wills, P. H. Andersson, P. Söderlind, and O. Eriksson, Phys. Rev. B **63**, 035103 (2000).
[16] J. Kunes, P. Novak, R. Schmid, P. Blaha, and K. Schwarz, Phys. Rev. B **64**, 153102 (2001).
[17] G. K. H. Madsen, P. Blaha, K. Schwarz, E. Sjöstedt, and L. Nordström, Phys. Rev. B **64**, 195134 (2001).
[18] C. Colinet and A. Pasturel, *Handbook on the Physics and Chemistry of Rare Earths*, edited by K. A. Gschneider Jr., L. Eyring, G. H. Lander, and G. R. Choppin (Elsevier Science B. V., North Holland, Amsterdam, 1994), Vol. 19.
[19] J. P. Perdew and Y. Wang, Phys. Rev. B **45**, 13 244 (1992).
[20] J. W. Connolly and A. R. Williams, Phys. Rev. B **27**, 5169 (1983).
[21] G. Robert, A. Pasturel, C. Colinet, and B. Siberchicot (unpublished).
[22] P. Villars and L. D. Calvert, *Pearson's Handbook of Crystallographic Data for Intermetallic Phases* (American Society for Metals, Metals Park, OH, 1985).